周波数選択性フェージングチャネルにおけるRCPTハイブリッドARQの特性評価

ガーグ・ディプシカ† 木村 良平† 安達 文幸‡

†‡東北大学大学院工学研究科電気通信工学専攻
〒980－8579 宮城県仙台市青葉区荒巻字青葉05

E-mail: †{deep,kimura}@mobile.ecei.tohoku.ac.jp, ‡adachi@ ecei.tohoku.ac.jp

あらまし 符号分割マルチアクセス（DS-CDMA）におけるレート可変パンクチャターボ符号（RCPT）のスループット特性を計算機シミュレーションにより明らかにしている．フレーム長，パンクチャレート，拡散率，アンテナ数，フェージングレート，伝搬路の電力遅延プロファイルなどがスループットにどのような影響を及ぼすかを考察している．1/8 程度までパンクチャした冗長ビットを再送するようにすれば最大のスループットが得られること，フレーム長やフェージングレートが小さくなるにつれスループットが低下するもののほとんど一定であることが分かった．また，拡散率を小さくするにつれてスループットは低下するものの実効伝送レート（スループット_kbps）は増加することが分かった．

Key words Hybrid ARQ, rate compatible punctured turbo codes, frequency selective channel, Rayleigh fading, mobile communications

Performance Evaluation of RCPT Hybrid ARQ Schemes for DS-CDMA Mobile Radio over Frequency Selective Rayleigh Fading Channel

Deepshikha GARG †, Ryohei KIMURA †, and Fumiyuki ADACHI ‡

†‡Department of Electrical and Communication Engineering,
School of Engineering, Tohoku University
Aza-Aoba 05, Aramaki, Aoba-ku, Sendai, 980-8579 Japan

E-mail: †{deep,kimura}@mobile.ecei.tohoku.ac.jp, ‡adachi@ ecei.tohoku.ac.jp

Abstract In this paper, we evaluate by computer simulations the throughput performance of the turbo-coded hybrid ARQ for direct sequence code division multiple access (DS-CDMA) with antenna diversity reception and Rake combining in a frequency selective Rayleigh fading channel. The effect of a range of system parameters and propagation parameters (viz., the frame length, puncturing rate, spreading factor, number of diversity antennas, fading rate, and the power delay profile of the multipath channel (number of paths and profile shape)) is investigated. It is found that the rate compatible punctured turbo (RCPT) coded hybrid ARQ system has the highest throughput when minimum amount of redundancy bits is transmitted with each retransmission and that the throughput is almost independent of the frame length and the fading rate. It is also found that smaller spreading factor for a given chip rate gives a higher throughput in bits/sec.

Key words Hybrid ARQ, rate compatible punctured turbo codes, frequency selective channel, Rayleigh fading, mobile communications

1. Introduction

In mobile radio communications, the received signal experiences multipath fading, which is produced by interference of many waves having different Doppler shifts created by reflections and refractions by nearby buildings surrounding a mobile station [1]. Since the propagation channel consists of numerous paths, the transmitted signal suffers from so-called frequency-selective multipath fading. Where high bit-rate transmissions are involved, the effects of frequency-selective fading cannot be ignored and the inter-symbol interference is produced. Hence, some error control techniques are necessary.

Conventional applications of forward error correction (FEC) coding usually consist of the utilization of fixed rate coding schemes which are the optimum for a given channel characteristics and results in acceptable error rates for the data to be transmitted. Turbo code [2], introduced in 1993 by Berrou et al., has been intensively studied as the error correction code for mobile radio applications. It has been found that the turbo code characteristics depend on a number of factors including the puncturing rate, frame length and the multipath fading rate [2-5]. However, to accommodate different error protection requirements, or to adapt to channel with unknown or time varying parameters, automatic repeat request (ARQ) schemes have been successfully employed.

In ARQ schemes [6], when an erroneous packet is detected, a retransmission request is sent to the transmitter until an error free detection is done. A simple ARQ scheme does not apply channel coding, while in hybrid ARQ schemes, channel coding for error correction is utilized. In type-II hybrid ARQ, a subset of hybrid ARQ schemes, the redundancy bits for error correction is adapted to the channel condition and retransmission of unnecessary bits is avoided.

Rate compatible punctured turbo (RCPT) codes in a hybrid ARQ scheme was proposed in [7] and shown to achieve enhanced throughput performance over an additive white Gaussian noise (AWGN) channel. In [8], it is shown that the throughput of RCPT hybrid ARQ scheme outperforms other ARQ schemes over fading and shadowing channels. However, to the best of authors' knowledge, the effect of the various system parameters and propagation parameters, e.g., the frame length, puncturing rate, spreading factor, fading rate, etc. on the throughput has not been fully evaluated.

In this paper, assuming direct sequence code division multiple access (DS-CDMA) [9], we evaluate the throughput performance of turbo coded hybrid ARQ schemes over frequency-selective Rayleigh fading channel with antenna diversity reception and Rake combining for various parameters, viz., the frame length, puncturing rate, spreading factor, number of diversity antennas, fading rate, and the power delay profile of the multipath channel (number of paths and profile shape). The evaluation is done by computer simulations firstly for ideal channel estimation and later compared with a practical channel estimation scheme called weighted multi-slot averaging (WMSA) channel estimation [10].

The remainder of this paper is organized as follows. Section II describes the structure of RCPT encoder and outlines the RCPT hybrid ARQ schemes considered in this paper. The computer simulation configuration and the mathematical model for the fading process are presented in section III. In section IV, the performance evaluation is done via computer simulations for various system parameters. Section V offers some conclusions and future work.

2. RCPT Coded Hybrid ARQ

2.1 Preliminaries of RCPT

The rate compatible punctured turbo codes consist of a turbo encoder-decoder and a puncturer-depuncturer.

The turbo encoder considered is a rate 1/3 turbo encoder with an S-ransom interleaver between the encoders. The resulting 3 sequences: systematic sequence $\{u_k\}$, and the two parity check sequences $\{p_k^{(1)}\}$ and $\{p_k^{(2)}\}$are punctured by the puncturer and stored in the buffer for possible retransmissions. A family of RCPT codes can be obtained by puncturing the 3 received sequences according to a puncturing pattern, which has a period P and is represented by $R ? P$ matrix, where the r^{th} row of the matrix denotes the puncturing pattern for the r^{th} bit stream (r=0~R-1).

The de-puncturer at the decoder side substitutes the unsent bits by a 0 and inputs the 3 sequences to the turbo decoder. The coherently detected received signal sample sequences associated with $\{u_k\}$, $\{p_k^{(1)}\}$, and $\{p_k^{(2)}\}$ are denoted by $\{y_k^{(u)}\}$, $\{y_k^{(p1)}\}$ and $\{y_k^{(p2)}\}$. The decoding algorithm for the turbo codes is a sub-optimal iterative algorithm [2, 11]. The turbo encoder/decoder parameters are shown in Table 1.

Table 1: Turbo encoder/decoder parameters

Encoder	Rate	Lowest rate 1/3
	Component encoder	(13,15) RSC
	Interleaver	S-random ($S=K^{1/2}$)
Decoder	Component decoder	Log-MAP
	Number of iteration	8

2.2 RCPT Hybrid ARQ

Type I and type II hybrid ARQ schemes are considered. The various hybrid ARQ schemes considered in this paper are obtained from the rate 1/3 (=1/R) turbo code by puncturing it with different puncturing period P.

2.2.1 Type I hybrid ARQ:

In the type I hybrid ARQ scheme considered in this paper, the two parity sequences obtained after turbo encoding are punctured with P=2 and transmitted along with the information sequence. If the receiver detects errors in the decoded sequence, a retransmission of that packet is requested. The retransmitted packet uses the same puncturing matrix as the previous packet. Instead of

discarding the erroneous packet, it is stored and combined with the retransmitted packet utilizing the time diversity (TD) effect [12].

2.2.2 Type II hybrid ARQ:

In type II hybrid ARQ, there are several variations. Type II hybrid ARQ *S-P-P* (systematic-parity1-parity2) scheme, only the systematic bits (sequence length of K bits) are transmitted in the first transmission. If error is detected, the parity bits obtained from the first RSC are transmitted. The parity bits and the systematic bits are together input to the decoder. Detection of error causes another retransmission request; the unsent parity bits from the second RSC are transmitted. Again, the previously received systematic bits $\{y_k^{(u)}\}$, and parity 1 bits $\{y_k^{(p1)}\}$ are used together with the newly received parity 2 bits $\{y_k^{(p2)}\}$ as a rate 1/3 code for decoding. The puncturing matrices used for the transmissions are:

$$\begin{bmatrix} 1 & 1 \\ 0 & 0 \\ 0 & 0 \end{bmatrix} \quad \begin{bmatrix} 0 & 0 \\ 1 & 1 \\ 0 & 0 \end{bmatrix} \quad \begin{bmatrix} 0 & 0 \\ 0 & 0 \\ 1 & 1 \end{bmatrix}$$

Presence of errors even after the third transmission causes the systematic bits, parity1 bits and parity 2 bits to be transmitted again as 4th, 5th, and 6th transmissions and the TD combining is employed.

Type II hybrid ARQ *S-P*2 [8] (systematic- puncture period *P*=2) is similar to the above scheme except that the sequences for the second and third transmissions are obtained after puncturing the parity 1 and parity 2 sequence with *P*=2. The puncturing matrices for the three transmissions are as follows:

$$\begin{bmatrix} 1 & 1 \\ 0 & 0 \\ 0 & 0 \end{bmatrix} \quad \begin{bmatrix} 0 & 0 \\ 1 & 0 \\ 0 & 1 \end{bmatrix} \quad \begin{bmatrix} 0 & 0 \\ 0 & 1 \\ 1 & 0 \end{bmatrix}$$

Type II hybrid ARQ *S-P*4 (systematic-puncture period *P*= 4) sends the systematic bits in the first transmission and successive retransmission consists of punctured sequences of length *K*/2 each, obtained from the two parity sequences with *P*=4. The 3?4 puncturing matrices are as follows:

$$\begin{bmatrix} 1 & 1 & 1 & 1 \\ 0 & 0 & 0 & 0 \\ 0 & 0 & 0 & 0 \end{bmatrix} \quad \begin{bmatrix} 0 & 0 & 0 & 0 \\ 1 & 0 & 0 & 0 \\ 0 & 0 & 0 & 0 \end{bmatrix} \quad \begin{bmatrix} 0 & 0 & 0 & 0 \\ 0 & 1 & 0 & 0 \\ 0 & 0 & 0 & 0 \end{bmatrix} \quad \begin{bmatrix} 0 & 0 & 0 & 0 \\ 0 & 0 & 1 & 0 \\ 0 & 0 & 0 & 0 \end{bmatrix} \quad \begin{bmatrix} 0 & 0 & 0 & 0 \\ 0 & 0 & 0 & 1 \\ 0 & 0 & 0 & 0 \end{bmatrix}$$

$$\begin{bmatrix} 0 & 0 & 0 & 0 \\ 0 & 0 & 1 & 0 \\ 0 & 0 & 0 & 0 \end{bmatrix} \quad \begin{bmatrix} 0 & 0 & 0 & 0 \\ 0 & 0 & 0 & 0 \\ 1 & 0 & 0 & 0 \end{bmatrix} \quad \begin{bmatrix} 0 & 0 & 0 & 0 \\ 0 & 1 & 0 & 0 \\ 0 & 0 & 0 & 0 \end{bmatrix}$$

The last scheme considered is the hybrid type II ARQ *S-P*8 (systematic puncture period *P*=8) [7,8]. The sequences to be transmitted in subsequent transmissions are obtained from the base 1/3 turbo code with the following 3?8 puncturing matrices (in octal notation):

$$\begin{bmatrix} 377 \\ 000 \\ 000 \end{bmatrix} \quad \begin{bmatrix} 000 \\ 200 \\ 002 \end{bmatrix} \quad \begin{bmatrix} 000 \\ 020 \\ 004 \end{bmatrix} \quad \begin{bmatrix} 000 \\ 010 \\ 100 \end{bmatrix} \quad \begin{bmatrix} 000 \\ 001 \\ 040 \end{bmatrix}$$

$$\begin{bmatrix} 000 \\ 301 \\ 030 \end{bmatrix} \quad \begin{bmatrix} 000 \\ 030 \\ 003 \end{bmatrix} \quad \begin{bmatrix} 000 \\ 003 \\ 020 \end{bmatrix} \quad \begin{bmatrix} 000 \\ 200 \\ 300 \end{bmatrix} \quad \begin{bmatrix} 000 \\ 020 \\ 002 \end{bmatrix}$$

The first transmission consists of *K* bits whereas successive transmissions consist of *K*/4 bits each. It should be noted that for the last two schemes, the size of successive transmissions is smaller than the first transmission. In all the schemes TD combining and code combing is utilized.

3. Computer Simulation Model

The throughput performance of the turbo-coded hybrid ARQ in a frequency selective Rayleigh fading channel with antenna diversity reception and Rake combining is evaluated by extensive computer simulations. A baseband equivalent transmission system model is illustrated in Fig. 3. The effect of a range of system and propagation parameters (viz., the frame length, puncturing rate, spreading factor, number of diversity antennas, fading rate, and the power delay profile of the multipath channel) is discussed.

3.1 Transmitter

The transmitter is composed of a CRC encoder, an RCPT encoder, a bit interleaver, a binary phase shift keying (BPSK) data modulator, and a BPSK spreading modulator. The CRC encoder adds error detection parity check sequence to a data sequence $\{d_{k'}\}$ of length K' to form a CRC coded sequence $\{u_k\}$ of length K. This sequence is input to the RCPT encoder where it is encoded by the turbo encoder and outputs a sequence $\{v_n\}$ of length N; $N=KR$ and the coded sequence is punctured and the resulting sequences are buffered for possible retransmissions. The sequence to be transmitted is block-interleaved and then data-modulated by BPSK. For the case when channel estimation is used, known N_p pilot symbols are time-multiplexed every N_d data symbols. N_p pilot symbols and succeeding N_d data symbols forms a slot of length $T_{\text{slot}}=(N_p+N_d)T$, where T is the BPSK symbol length. The resulting sequence is represented as $\{v'_{n'};\ n'=0\sim N'-1\}$, where $N'=N(1+N_p/N_d)$. Spreading is implemented by multiplying the pilot-inserted BPSK sequence with the long pseudo random (PN) sequence $c(t)$ having chip period T_c. The DS-spread signal $s(t)$ can be expressed in a baseband equivalent representation as

$$s(t) = \sqrt{2S}\,v'(t)c(t) \quad , \qquad (1)$$

$$\text{with} \quad \begin{aligned} v'(t) &= \sum_{k=-\infty}^{\infty} \exp[j\theta(k)]u(t/T - k) \\ c(t) &= \sum_{q=-\infty}^{\infty} pn(q)u(t/T_c - q) \end{aligned} \quad , \qquad (2)$$

where S denotes the average signal power, $v'(t)$ represents the BPSK symbol sequence waveform, and $c(t)$ the spreading sequence waveform. In Eq. (2), $\{pn(q)\}$ represents the long PN spreading sequence with chip length of T_c, $\theta(k) = 0(\pi)$ for $v'_k=1(0)$ is the BPSK-modulation phase, and $u(t)$ is the rectangular pulse with $u(t)=1$ $(0 \le t \le 1)$ and 0 (otherwise). The spreading factor (SF) is defined as the ratio of the BPSK symbol length T and the chip length T_c and is given by $\text{SF}=T/T_c$.

3.2 Propagation Channel Model

The DS-spread signal is transmitted via a propagation channel and received by M antennas. It is assumed that the propagation channel is frequency- selective and has L discrete paths having different time delays (multiple of

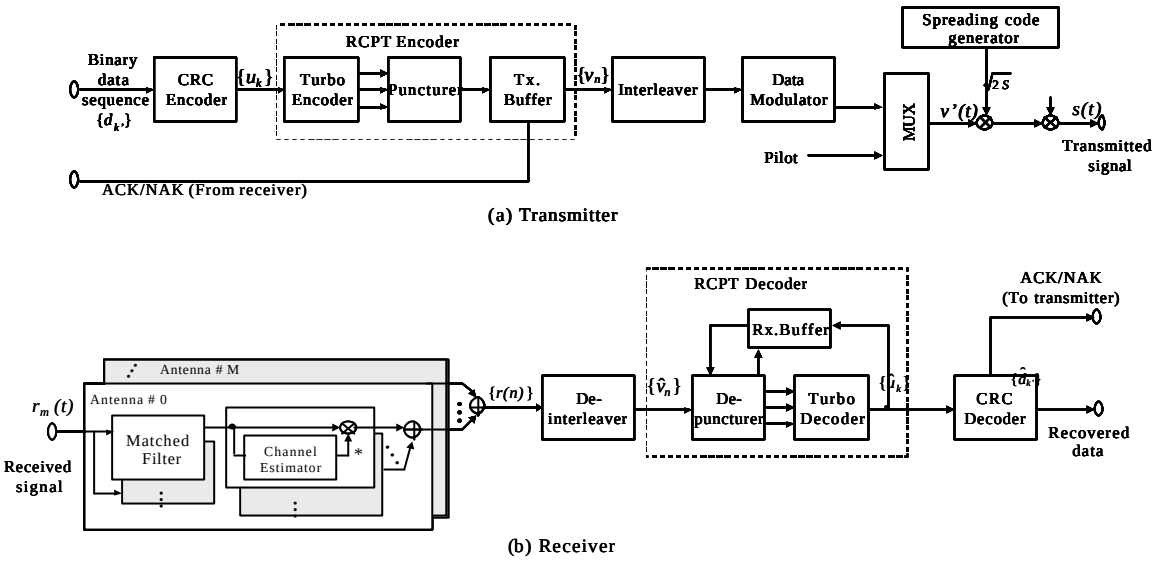

Figure 1: System model.

T_c) and experiencing independent Rayleigh fading. The channel impulse response $h_m(t,?)$, seen on the m^{th} antenna, m=0,..., M-1, can be expressed as [13]

$$h_m(t,?) ? \sum_{l?0}^{L?1} ?_{m,l}(t)?(? ? ?_l) \quad , (3)$$

where $?_{m,l}(t)$ and $?_l$ denote the complex fading channel gain and time delay of the lth path, respectively, with $\mathbf{E}[\sum_{l?0}^{L?1} |?_{m,l}(t)|^2] ? 1$, with E[.] being the ensemble average operation. It is assumed that $\{?_{m,l}(t)$; m=0~M-1, l=0~L-1$\}$ are independent identically distributed (iid) complex Gaussian processes. The power delay profile is shown in Fig. 2. $\mathbf{E}[|?_{m,l}(t)|^2]$, $l ? 0 \sim L ? 1$, are assumed to be exponentially decreasing with coefficient "$?$" and exponent "$?$", where "$?$" is given by $? ? [1 ? \exp(??)] / [1 ? \exp(?L?)]$.

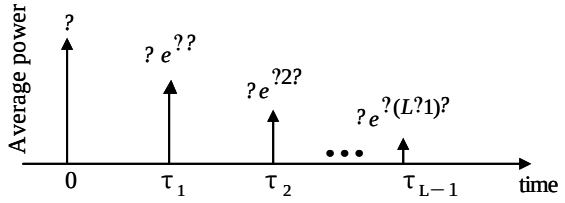

Figure 2: Power delay profile.

3.3 Receiver

As shown in Fig. 1, the DS-CDMA Rake receiver consists of a matched filter (MF), a coherent demodulator, a bit de-interleaver, an RCPT decoder and a CRC decoder. The low-pass equivalent of the received signal seen on the m^{th} receive antenna can be expressed as

$$r_m(t) ? \sum_{l?0}^{L?1} ?_{m,l}(t)s(t ? ?_l) ? n_m(t) \quad , (4)$$

where $n_m(t)$ denotes the AWGN with single-sided power spectrum density of N_0. The received faded DS-spread signal is resolved into L copies of transmitted BPSK signal sequence by the MF. The MF consists of L correlators; each correlator multiplies $r_m(t)$ with the locally generated spreading sequence waveform $c(t)$, which is time-synchronized to the time delay of each propagation path, and integrates over one BPSK symbol period. Perfect knowledge of propagation time delays is assumed in this paper. The MF output sample $r_{m,l}(n)$ at the nth symbol time position, associated with the lth path, is represented as

$$r_{m,l}(n) ? \int_{nT??_l}^{(n?1)T??_l} r_m(t)c(t ? ?_l)dt \\ ? \sqrt{2S}?_{m,l}(n)\exp[\,j?(n)] ? w_{m,l}(n) \quad , (5)$$

where $?_{m,l}(n) ? ?_{m,l}(nT)$, for simplicity, is assumed to be constant over a symbol duration, and $w_{m,l}(n)$ represents the noise component owing to the AWGN.

The channel estimate $\tilde{?}_{m,l}(n)$ is computed by the WMSA algorithm and coherent demodulation carried out. For antenna diversity reception, maximum ratio combining (MRC) is assumed as it was found to be ideal for turbo decoding [14]. Assuming the L fingers, the Rake combiner output r(n) can be represented as

$$r(n) ? \sum_{m?0}^{M?1} \sum_{l?0}^{L?1} r_{m,l}(n)\tilde{?}^{\,?}_{m,l}(n) \quad , (6)$$

where * denotes the complex conjugate. The pilot-extracted sequence of $r(n)$ is de-interleaved to obtain the Turbo coded sequence $\{\hat{v}_n\}$, which is fed to the RCPT decoder to recover the CRC coded sequence $\{\hat{u}_k\}$. If no error is detected, the CRC decoder outputs the data sequence $\{\hat{d}_{k'}\}$ as the received data. In the case of errors being detected by the CRC decoder, a retransmission is requested. An error-free reverse channel and perfect error detection using CRC are assumed throughout the paper.

4. Computer Simulation Results

The computer simulation parameters are summarized in Table 2. In Table 2 and henceforth, frame length is the information sequence length (K) that is input to the turbo encoder. The turbo encoder/decoder parameters are as shown in Table 1. The chip rate is kept constant at 4.096M chips/sec (cps). Uncorrelated, time-varying Rayleigh fading paths are generated using Dent's model [15]. In the following simulations, unless otherwise stated, the spreading factor is taken to be SF=32, resulting in a transmission bit rate of 128kbps, and the fading maximum Doppler frequency f_D is taken to be 128Hz, corresponding to a carrier frequency of 2GHz and a vehicle speed of 70km/hr, the number of paths and the number of diversity antennas are taken to be L=1~4 and M=1~4, respectively, and the propagation time delay difference between the nearest two paths is taken to be 1 chip. As a summary, the following parameters are used unless otherwise stated: frame length=1024bits, SF=32, L=4, ? =0, $f_D T_c$=1/32000, and no antenna diversity (M=1). Comparison is done for ideal channel estimation and K=2 WMSA channel estimation. The tap weight vectors for K=2 WMSA are taken to be (0.6, 1.0, 1.0, 0.6) [10].

In all the simulation results, throughput efficiency ? is defined as

$$? \; ? \; \frac{Bits \;\; transmitted \;\; successfully}{Total \;\; number \;\; of \;\; bits \;\; transmitted} \quad . \; (7)$$

Table 2: Simulation condition

Chip rate	4.096 Mcps	
Information rate	128kbps- 1.024Mbps	
Channel coding	Turbo code	
Channel interleaver	Block Interleaver	
Spreading factor	1-32	
Spreading sequence	Long random sequence	
Modulation	Data	BPSK
	Spreading	BPSK
Frame length	128-1024 bits	
Slot structure	Pilot symbols: 4 Information symbol: 32	
Channel model	Forward	Frequency selective Rayleigh fading
	Reverse	Ideal
Antenna diversity	MRC	
Maximum number of transmissions	100	

4.1 Comparison of various hybrid ARQ schemes

The throughput efficiency for the different hybrid schemes presented in Section II is plotted in Fig. 3 as a function of the average received energy per coded bit per antenna-to-AWGN power spectral density ratio (E_b/N_0). For reference, the throughput for basic ARQ scheme (i.e., no coding) is also plotted.

From Fig. 3 it is seen that the type I hybrid ARQ scheme gives an improved throughput performance, compared to the basic ARQ scheme, at lower E_b/N_0 ratio (the average number of transmissions is almost always 1); however due to the redundancy bits added (1 check bit for every information bit), the throughput can never rise beyond 0.5 no matter how good the channel condition is. On the other hand, in the type II hybrid ARQ schemes, redundancy bits are transmitted only on request. This ensures that a throughput of 1 may be reached when channel condition is good although the average number of transmissions is higher than the type I hybrid ARQ scheme.

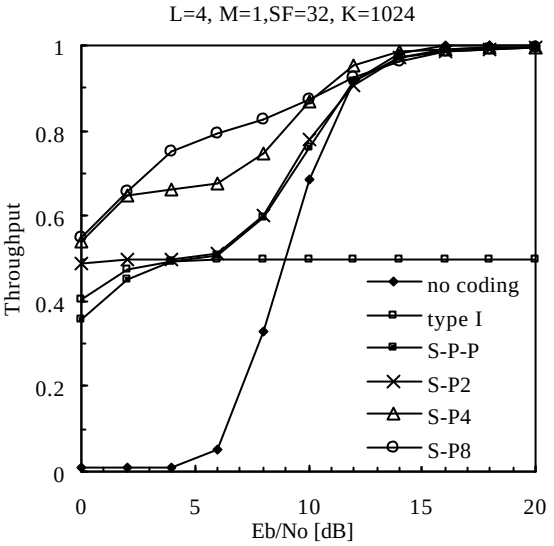

Figure 3: Comparison of Hybrid ARQ schemes.

For the type II hybrid ARQ schemes, the throughput is the best for the *S-P*8 while the average number of transmissions is lowest for the *S-P*2 scheme. In the 2dB< E_b/N_0<8dB region a flatness is observed in the throughput curve. In this region, the first transmission (systematic bits) is in error and a retransmission request is sent. This causes the check bits (punctured bits from parity 1 and parity 2) to be sent. However, almost always the second transmission is enough for error correction. This is the reason why the throughput curve has a flat region. The flatness of the curve is still seen in the *S-P*4 scheme but has been reduced to a great extent in the *S-P*8 scheme. Since the *S-P*8 scheme was found to give the best throughput performance, it has been used to evaluate the effect of other system parameters.

4.2 Effect of frame length

Fig. 4 plots the throughput performance for different frame lengths for no antenna diversity (M=1), SF=32, and $f_D T_C$=1/32000. In the original paper on turbo codes by Berrou et al. [2], and many of the subsequent papers, impressive results have been presented for coding with very large frame lengths of the order of 16384 bits. The BER degrades rapidly for shorter frame length. Longer length packets are vulnerable to the channel, but turbo coding is more robust in the case of longer frame length. However, since the probability of frame error can be generally reduced according to the decrease in frame length, ARQ schemes are better suited for shorter frame length. The throughput obtained for different E_b/N_0 is plotted as a function of the frame length in Fig. 4. It is seen that in the case of ideal channel estimation, the throughput is almost insensitive to the frame length. When E_b/N_0=8dB, the throughput efficiency slightly

decreases as the frame length increases beyond 256 bits per frame.

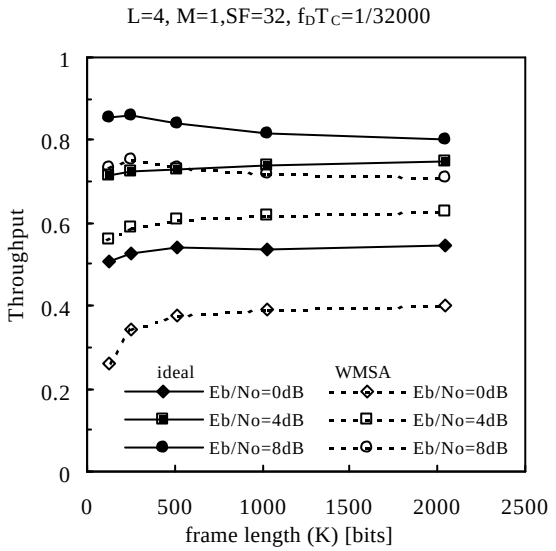

Figure 4: Effect of frame length.

When WMSA channel estimation technique is used, the throughput decreases owing to the channel estimation error and the addition of pilot symbols.

4.3 Effect of spreading factor

Figure 5 plots the throughput as a function of SF with E_b/N_0 as parameter. The throughput is more or less independent of the SF for SF ? 8 . For smaller SF, the throughput decreases due to increasing inter-path interference (IPI), however, the throughput of 0.37 can still be achieved at E_b/N_0=0dB even when SF=1. On the other hand, according to our other computer simulation in the case of no coding, the throughput rapidly decreased as the SF decreased and is nearly zero when SF=1. The dependence of throughput on spreading factor is similar in the case of WMSA channel estimation, as well. However, compared to the ideal channel estimation case, the throughput falls due to the presence of channel estimation error and non-information bearing pilot symbol insertion (throughput reduction only due to pilot insertion is 11%). When SF=64, the throughput at E_b/N_0=8dB reduces by 15% (from 0.83 to 0.71) owing to channel estimation error, whereas the reduction at E_b/N_0=0dB is 27% (from 0.55 to 0.4). When SF=1, the reduction is by about 30%(45%) at E_b/N_0=8dB(0dB). This larger reduction in the throughput for smaller SF is due to increased channel estimation error.

For high-speed communications, lowering the SF may be advantageous as it allows higher rate data transmission for a fixed chip rate at the cost of retransmissions of few extra bits. Increased data rate is a direct consequence of decreased SF when chip rate is kept constant. Here a new throughput in bits/sec (bps) is defined as

$$? \; ? \; data \;\; rate \; ? \; \frac{bits \;\; transmitte d \;\; successful ly}{total \;\; number \;\; of \;\; bits \;\; transmitte d} \quad . \quad (8)$$

It is found from Fig. 5(b) that the throughput in bps increases as the spreading factor decreases; the use of SF=1 (no spreading) achieves the highest throughput in kbps of 2400 kbps at E_b/N_0 of 8dB, with ideal channel estimation. A possible reason for this is qualitatively explained below. The receiver consists of a Rake receiver with L fingers, each perfectly synchronized to its corresponding path. Therefore, the Rake combiner can be viewed as a selection combiner that selects the best path having the maximum path gain. This stops the throughput from falling to zero despite of SF=1. The use of SF=1 offers an 8 times faster transmission rate compared to the use of SF=8; the result is an increased throughput in kbps.

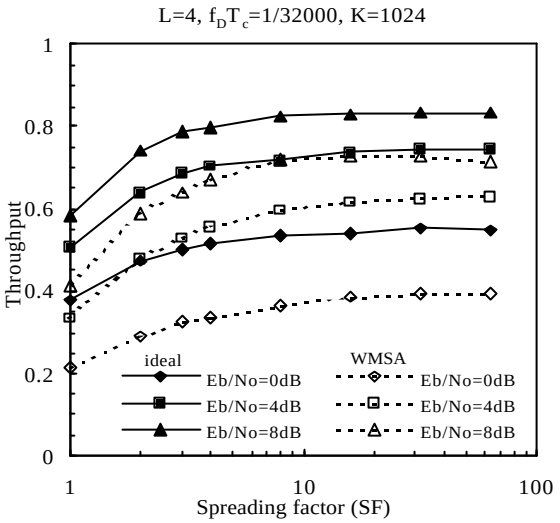

(a) Throughput defined by Eq. (7)

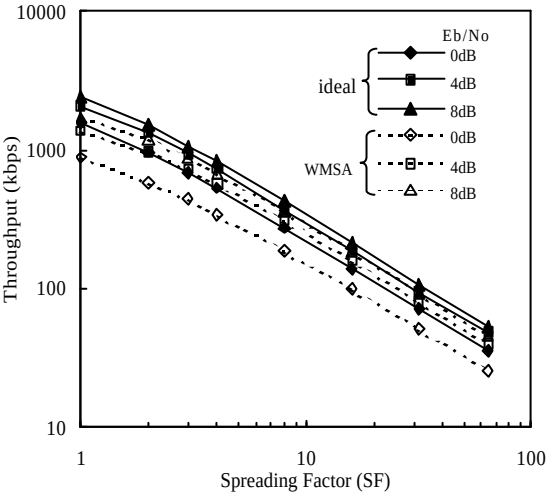

(b) Throughput in kbps defined by Eq. (8)

Fig. 5: Effect of spreading factor.

4.4 Effect of the number of diversity antennas

Figure 6 plots the throughput as a function of E_b/N_0 with the number M of antennas as a parameter. The throughput increases with the increase in the number of antennas. For ideal channel estimation, flatness in the curves is seen at throughput around 0.8 except for no antenna diversity (M=1). The first transmission consists of only the systematic bits and the turbo decoder is not

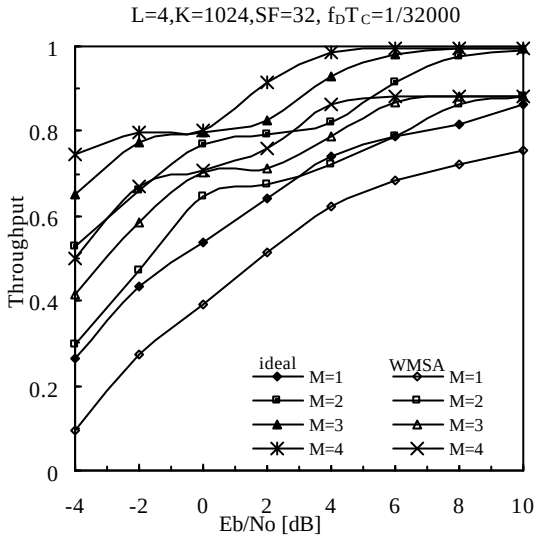

Figure 6: Effect of the number of diversity antennas.

utilized. So, even when the number of antennas is increased, there usually is a retransmission request for the parity bits. For M=2, in the region $0\text{dB} \leq E_b/N_0 \leq 4\text{dB}$, the number of transmissions is about 2 and hence the throughput remains almost constant. It is also found from the Fig. 6 that at E_b/N_0=0dB the throughputs for M=2, 3 and 4 are nearly same.

4.5 Effect of fading maximum Doppler frequency

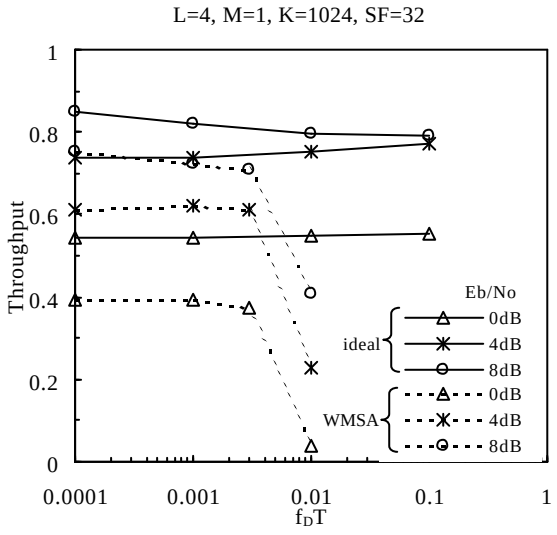

Figure 7: Effect of maximum Doppler frequency.

The maximum Doppler frequency normalized by the bit length T is denoted by f_DT. Smaller value f_DT corresponds to slow vehicular velocity and vice versa for the given spreading factor and chip rate. Figure 7 plots the throughput for *S-P*8 hybrid type II ARQ scheme as a function of f_DT for various E_b/N_0 values (here, M=1, L=4 and frame length=1024). It is known that the faster the fading, the better is the interleaving effect and hence the higher is the coding gain. However, the throughput is found to be almost insensitive to the f_DT value. This is because the small coding gains of turbo code for smaller f_DT value are offset by the burst error property, which is favorable for ARQ.

As discussed earlier when the WMSA channel estimation scheme is used, the throughput decreases owing to the channel estimation error and the insertion of pilot symbols. It is seen from Fig. 7 that the throughput stays more or less constant for f_DT less than 0.003, however it decreases drastically when f_DT approaches 0.01. In this case, the maximum Doppler frequency normalized by the slot length f_DT_{slot} becomes 0.36, which is too large for K=2 WMSA channel estimation to estimate the channel gain (the slot length T_{slot} is 36T for N_p=4 pilots and N_d=32 data symbols). So, for higher f_DT, the WMSA channel estimation scheme should be replaced by a better channel estimator that is robust in fast fading channels, e.g., [16].

4.6 Effect of the delay profile shape

The effect of the power delay profile shape of the propagation channel on the throughput performance is plotted in Fig. 8 as a function of E_b/N_0 with the number L of paths as parameter. In a frequency-selective Rayleigh fading channel, there exists more than one path. To take advantage of this fact, the receiver is equipped with a Rake combiner. It is seen from Fig. 8 that as the number of paths increases from one to two, the throughput increases; yet further increase in the number of paths does not change the performance. When the WMSA channel estimation scheme is utilized, the degradation in performance is worse for the case when L=4 than when L=2. This is due to the reduced power of each path that is insufficient for good channel estimation.

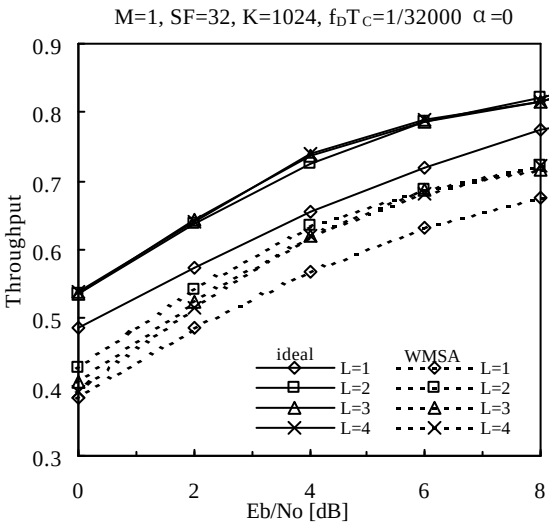

Figure 8: Effect of power delay profile shape.

For the given value of L, α=0 corresponds to equal power distribution among the paths (or uniform power delay profile) and $\alpha = \infty$ corresponds to one path. It was found that the best throughput is obtained when α=0. As α increases, the performance approaches to that of L=1 when ideal channel estimation is assumed. However, with WMSA channel estimation, for very high α, the

throughput is lower than that of one path. This is because the Rake combiner assumed in this paper always assumes L=4 paths and thus, for high ?, channel estimation for the weak paths is inaccurate and results in increasing BER more than the L=1 case (notice that if only strong paths are used for Rake combining, better throughput performance can be achieved). It was also found that the time delay difference between the paths has no effect on the throughput.

5. Conclusion

In this paper, we presented a comprehensive performance evaluation of the turbo coded hybrid ARQ in a frequency-selective Rayleigh fading channel for various system parameters like the frame length, the fading rate, the spreading factor, and propagation parameters (the power delay profile shape of the multipath channel and the number of diversity antennas). The evaluation was done for ideal channel estimation and practical channel estimation, i.e., WMSA channel estimation, for comparison. From the detailed evaluations presented in this paper, we can draw the following conclusions.

(a) The turbo-coded hybrid ARQ has the highest throughput when minimum amount of redundancy bits is transmitted with each retransmission, i.e., the puncturing period for the parity sequences is 8.

(b) The throughput is almost insensitive to the frame length. This is because the decreasing throughput due to increasing probability of frame error for longer frame length is offset by the increasing turbo coding gain.

(c) The throughput in bits/sec is higher for lower SF even though the throughput efficiency is lower due to the stronger effect of IPI for the single user case.

(d) The performance improves with the increase in the number of diversity antennas. However, the improvement in performance obtained with increasing number of antennas decreases as the number of antennas increases.

(e) For ideal channel estimation, the throughput is almost independent of $f_D T$; however when practical channel estimation is employed, the performance degrades for fast fading rate.

(f) The performance improves when the number of paths increases from 1 to 2, but further increase in paths does not improve the performance.

In a DS-CDMA system, spreading factor is a very important design parameter that sets the transmission data rate for the given chip rate. From the results obtained in this paper, it can be said that if a method is designed to remove the inter-path interference, the data rate can be further increased. Also interesting is the investigation of adaptive rate compatible turbo coded hybrid ARQ adapted to changing channel conditions.

References

[1] W. C., Jakes Jr., Ed., *Microwave mobile communications*, Wiley, New York, 1974.

[2] C. Berrou, A. Glavieux, and P. Thitimajshima, "Near Shannon limit error-correcting coding and decoding - Turbo codes", Proc. Int. Conf. Communications, pp. 1064-1070, May 1993.

[3] J. P. Woodard and L. Hanzo, "Comparative study of turbo decoding techniques: an overview", IEEE Trans. Vehicular Technology, Vol. 49, No. 6, pp. 2208-2233, Nov 2000.

[4] J. Hagenauer, E. Offer, and L. Papke, "Iterative decoding of binary block and convolutional codes", IEEE Trans. Information Theory, Vol. 42, No. 2, pp. 429-445, March 1996.

[5] D. Divsalar and F. Pollara, "Turbo-Codes for PCS Applications", Proc. Int. Conf. Communications, Seattle, WA, pp. 54-59, Jun. 1995.

[6] S. Lin and D. J. Costello, Jr., *Error control coding: Fundamentals and applications*, Prentice Hill, 1983.

[7] D. N. Rowitch and L. B. Milstein, "Rate compatible punctured turbo (RCPT) codes in hybrid FEC/ARQ system", Proc. Comm. Theory, Mini-conference of GLOBECOM'97, pp. 55-59, Nov. 1997.

[8] T. Ji and W. E. Stark, "Turbo-coded ARQ schemes for DS-CDMA data networks over fading and shadowing channels: throughput, delay and Energy efficiency", IEEE Journal on Selected Areas in Communication, Vol. 18, pp. 1355-1364, Aug. 2000.

[9] A. J. Viterbi, *CDMA: Principles of Spread spectrum communications*, Addison-Wesley, June 1995.

[10] H. Andoh, M. Sawahashi, and F. Adachi, "Channel estimation filter using time-multiplexed pilot channel for coherent RAKE combining in DS-CDMA mobile radio", IEICE Trans. Commun., Vol. E81-B, pp. 1517-1526, July 1998.

[11] L. R. Bahl, J. Cocke, F. Jelinek, and J. Raviv, "Optimal decoding of liner codes for minimizing symbol error rate", IEEE Trans. Information Theory, pp. 284-287, March 1974.

[12] F. Adachi, S. Ito, and K. Ohno, "Performance analysis of a time diversity ARQ in land Mobile radio", IEEE Trans. Communications, Vol. 37, pp.177-183, Feb. 1989.

[13] C. Kchao and G. L. Stuber, "Analysis of a direct-sequence spread-spectrum cellular radio system," IEEE Trans. Commun., Vol. 41, pp. 1507-1516, Oct. 1993.

[14] D. Garg, R. Kimura, and F. Adachi, "Combined effect of turbo coding and multichannel reception in a Rayleigh fading channel," (in Japanese) The 442th Transmission Eng. Colloquium, Tohoku University, June 2001.

[15] P. Dent, G. E. Bottomley, and T. Croft, "Jakes fading model revisited", Electronics Letters, Vol. 29, No. 13, June 1993.

[16] S. Takaoka and F. Adachi, "Pilot-aided adaptive prediction channel estimation in a mobile radio," (in Japanese) The 441th Transmission Eng. Colloquium, Tohoku University, May 2001.